

Characterization of Kraft Lignin Prepared from Mixed Hardwoods by 2D HMQC and ^{31}P NMR Analyses

Ji Sun Mun,^a Justin Alfred Pe III,^b and Sung Phil Mun^{b,*}

This study was conducted to determine the lignin substructures, hydroxyl (phenolic + aliphatic) contents, and carboxyl contents in kraft lignin (KL) prepared from mixed hardwoods by using 2D Heteronuclear Multiple Quantum Coherence Nuclear Magnetic Resonance (HMQC NMR) and ^{31}P NMR techniques. Based on 2D HMQC NMR analysis of KL, stilbene and vanillin substructures were present in the aromatic region, while trace amounts of β -O-4 and β - β moieties were detected in the oxygenated aliphatic region. The total hydroxyl content calculated from ^{31}P NMR was 5.24 mmol/g KL. The aliphatic hydroxyl content was 1.04 mmol/g KL, and phenolic hydroxyl content was 4.20 mmol/g KL. Of the phenolic hydroxyl groups, the contribution of syringyl (S) and guaiacyl (G) was 1.02 and 0.97 mmol/g KL, respectively. The S/G molar ratio of KL calculated from ^{31}P NMR was 1.05. The carboxyl content was 0.44 mmol/g KL.

DOI: 10.15376/biores.17.4.6626-6637

Keywords: Kraft lignin; Mixed hardwood; HMQC; ^{31}P NMR; Hydroxyl content

Contact information: a: Department of Carbon Materials and Fiber Engineering, Jeonbuk National University, 54896, Jeonju, Korea; b: Department of Wood Science and Technology, Jeonbuk National University, 54896, Jeonju, Korea; *Corresponding author: msp@jbnu.ac.kr

INTRODUCTION

The road to carbon neutrality by 2050 is considered as the world's most urgent mission (Guterres 2020). Interest in the utilization of bioresources such as lignin, the second most abundant organic materials next to cellulose, are growing and actively studied. Among all types of lignin, kraft lignin (KL) is considered as an attractive yet underutilized bioresource to researchers and pulping companies. Valorization of lignin for industrial applications has been challenging due to their heterogeneity, modified structure, presence of sulfur, and poor quality of the final product (Vishtal and Kraslawski 2011; Jardim *et al.* 2020). Despite these drawbacks, KL still has potential to be converted into value-added materials, as it is cheap, renewable, and available in large amounts (Mun *et al.* 2021).

Previously, commercial KL produced from South Korea was characterized by elemental analysis, gel permeation chromatography, infrared spectroscopy, and ^1H and ^{13}C NMR spectroscopy. The structural changes that occurred in KL have been compared to milled wood lignins (MWLs), which were prepared from the same hardwood species used in the production of KL. In general, 1D NMR provides structural information such as the bond between atoms and functional groups. In the case of lignin, different types of linkages present in lignin can be identified from ^1H and ^{13}C NMR. Because lignin is an amorphous polymer, severe overlapping of peaks is inevitable. The advantage of 2D NMR methods such as HMQC is that they can detect the direct chemical bonds between hydrogen and carbon in a molecule by detecting the correlation between ^1H and directly spin-bonded,

heterogeneous nucleus, ^{13}C (Yu *et al.* 2003). With this, HMQC analysis of KL from mixed hardwoods was performed since the linkages in lignin substructures can be determined more clearly through 2D NMR analysis (Wen *et al.* 2013a).

In lignin chemistry, the structural features in lignin that indicate reactivity are the phenolic hydroxyl groups (Cateto *et al.* 2008). Thus, the determination of phenolic hydroxyl groups in KL is necessary for their future application and utilization. Techniques such as ultraviolet (UV), infrared (IR), and ^1H NMR spectroscopy have been reported for the analysis of hydroxyl groups in lignin (Argyropoulos *et al.* 2021). Through UV spectroscopy, only phenolic hydroxyl groups can be determined (Goldschmid 1954). Quantitative information on hydroxyl groups cannot be obtained from IR spectroscopy due to the signal overlapping issues. ^1H NMR can quantify the aliphatic and phenolic hydroxyl groups after acetylation of lignin. ^{31}P NMR is capable of precisely detecting and quantifying the different hydroxyl groups such as syringyl (S), guaiacyl (G), *p*-hydroxyphenyl (H), and even carboxyl groups in lignins (Argyropoulos *et al.* 2021).

In this work, the lignin substructures and hydroxyl groups of KL, prepared from mixed hardwoods, were determined *via* 2D HMQC and ^{31}P NMR techniques. The outcomes gave a better understanding of the structural features of hardwood KL, which can be useful for chemical modification, functionalization, and utilization of KL in the near future. In addition, this work adds to the literature for hardwood KLS since most of studies focused on softwood KL.

EXPERIMENTAL

Materials

The KL used in this study was provided by Moorim P&P Co., Ltd. located in Ulsan, Korea. The wood chips used for kraft pulping were 50% *Acacia* spp. from Vietnam and 50% mixed hardwood (*Quercus* spp. + other hardwood, 1:1) from Korea. A detailed description about the cooking conditions and purification process of KL can be found in Mun *et al.* (2021).

The reagents used for acetylation were anhydrous pyridine (99.5%, Kanto Chemical, Tokyo, Japan) and acetic anhydride (93%, Duksan Pure Chemical, Ansan, Korea). The solvents used for 2D HMQC NMR were acetone- d_6 (Cambridge Isotope Laboratories, Andover, USA) and D_2O (Merck, Darmstadt, Germany). The reagents used for ^{31}P NMR were anhydrous pyridine (99.5%, Kanto Chemical, Tokyo, Japan), CDCl_3 (Eurisotop, Saint-Aubin, France), *N*-hydroxy-5-norbornene-2,3-dicarboximide (97%, AlfaAesar, Lancashire, UK), chromium (III) acetylacetonate (97%, AlfaAesar, Ward Hill, USA), and 2-chloro-4,4,5,5-tetramethyl-1,3,2-dioxaphospholane (95%, Sigma-Aldrich, St. Louis, USA). All reagents and solvents were used without further purification. Molecular sieves with pore diameter 4 Å (1.6 mm pellet, Yakuri Pure Chemicals, Osaka, Japan) were used for all experiments.

2D HMQC NMR Analysis

For the HMQC NMR analysis, the sample was firstly acetylated with anhydrous pyridine and acetic anhydride (1:1 v/v) at room temperature for 48 h according to the authors' previous paper (Mun *et al.* 2021). A 100 mg acetylated KL (Ac-KL) was dissolved in 150 μL acetone- d_6 and 300 μL D_2O (1:2 v/v) solvent in a 10-mL conical beaker. The conical beaker was sonicated for 1 to 2 min to dissolve the sample. The mixture was filtered

through a fine glass wool suspended inside a Pasteur pipette, which was directly connected to an NMR tube. The conical beaker was rinsed with solvent, and the contents were transferred as described in the previous filtration method. The measurement was conducted using an NMR spectrometer (500 MHz, JEOL, Tokyo, Japan) at the Center for University-wide Research Facility (CURF), Jeonbuk National University (JBNU), Jeonju, Korea.

³¹P NMR Analysis

The hydroxyl content of KL was determined by ³¹P NMR analysis according to the method of Argyropoulos *et al.* (2021). The pyridine/CDCl₃ (1.6:1 v/v) solvent was prepared by mixing 6.40 mL anhydrous pyridine and 4.00 mL CDCl₃ in a pre-dried 20-mL vial. Molecular sieves were added into the vial to completely remove moisture. The vial was sealed with a septum cap and stored in the dark. The internal standard, *N*-hydroxy-5-norbornene-2,3-dicarboximide (NHND, 35.8 mg), and the relaxation agent, chromium (III) acetylacetonate (10 mg), were dissolved in 280 μL pyridine/CDCl₃ solvent in a pre-dried 2-mL vial. Molecular sieves were added into the internal standard (IS) solution. The vial was sealed with a septum cap and wrapped with an Al foil. A 30 mg vacuum-dried moisture-free KL was dissolved in 500 μL pyridine/CDCl₃ solvent in a pre-dried 2-mL vial. This was followed by the addition of 100 μL IS solution *via* syringe. The vial was sonicated for 90 s and then stirred at around 500 rpm for 18 h using a magnetic stirrer (RCN-7, Eyela, Tokyo, Japan). After dissolution of KL, 100 μL phosphitylating agent, 2-chloro-4,4,5,5-tetramethyl-1,3,2-dioxaphospholane (TMDP), was added into the vial using a syringe and then stirred vigorously under magnetic stirring. The sample was transferred to an NMR tube using the same filtration method above. The ³¹P NMR analysis was conducted using an NMR spectrometer (600 MHz, JEOL, Tokyo, Japan) at the CURF, JBNU. The spectrum was acquired through an inverse-gated decoupling pulse sequence, 10 s relaxation delay, and 64 scans.

RESULTS AND DISCUSSION

2D HMQC NMR Analysis

The ¹³C NMR spectra of acetylated KL (Ac-KL) and non-acetylated KL were compared. The ¹³C NMR spectra shown in Fig. 1 were obtained from HMQC analysis (Ac-KL) and the previous study (KL). The chemical shifts are listed in Table 1 along with their assignments in acetylated lignins based on Nimz *et al.* (1981). In Ac-KL, two strong signals at 171 to 168 and 20.6 ppm correspond to the C=O and CH₃ in acetyl groups, respectively. Since these two signals were absent in the spectrum of KL, these confirmed that the hydroxyl groups in KL were well acetylated.

The 160 to 100 ppm in ¹³C NMR spectrum corresponds to the aromatic region and 90 to 50 ppm (excluding the methoxyl group signal) to the aliphatic region (Nimz *et al.* 1981; Zhao *et al.* 2017). In the aromatic region, syringyl (S) and guaiacyl (G) related signals were present as anticipated for hardwood lignins (Ralph *et al.* 2007; Katahira *et al.* 2018). The number assignments in the ¹³C NMR of Ac-KL refers to the substructures shown in Fig. 2. In case of Ac-KL, one of the most remarkable signals in the aromatic region was **3**; this signal was assigned to the S_{3,5} and G₃ units. This corresponded to the carbon containing the methoxyl groups. Also, relatively strong signals **8** and **11** were assigned to G₅ and S_{2,6} units, respectively, which corresponded to the free aromatic C–H bonds. Meanwhile, the weak signals found in the aliphatic region of both Ac-KL and KL

were indications of aliphatic sidechain cleavage.

In ^{13}C NMR spectrum of KL, two distinct signals at 148.2 ppm and 115.5 ppm were not detected in Ac-KL. The intense signal at 148.2 ppm corresponded to $\text{S}_{3,5}$ and G_3/G_3' units; the biphenyl (5-5₃) was also assigned to this signal (Mun *et al.* 2021, Fig. 2). Thus, the signal at 148.2 ppm in KL shifted to 153.2 ppm in Ac-KL. The signal at 115.5 ppm was attributed to G_5 overlapping with $\text{H}_{3,5}$. This suggested that the signal at 115.5 ppm in KL shifted to 123.6 ppm in Ac-KL.

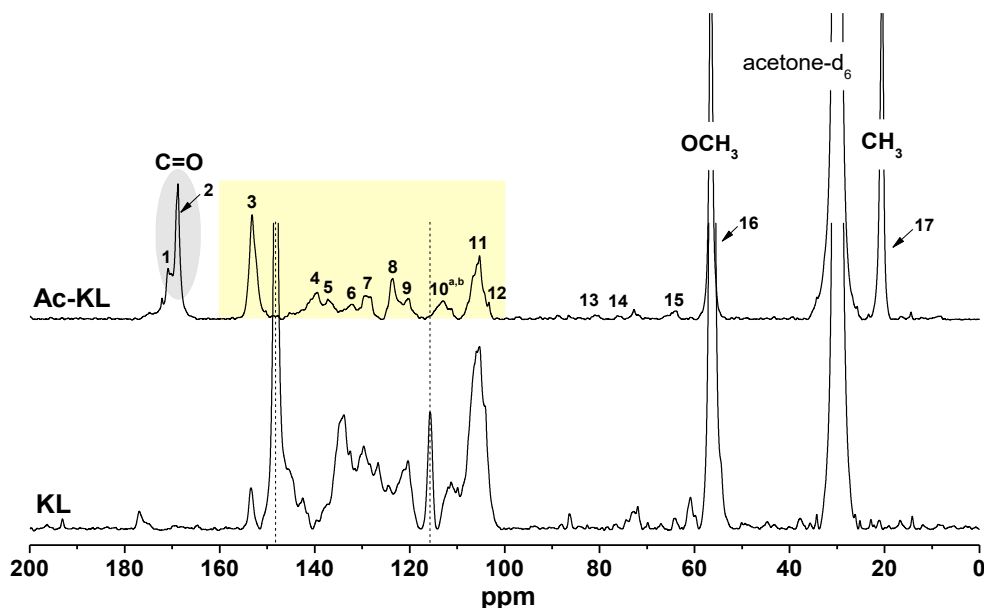


Fig. 1. ^{13}C NMR spectra of Ac-KL and KL

Table 1. ^{13}C NMR Assignments of Ac-KL

Signal No.	Chemical Shift (ppm)	Assignment
1	170.9	CO in acetates of primary alcohols
2	168.8	CO in acetates of phenols
3	153.2	ac $\text{G}_3(\alpha\text{-OR})$, ac $\text{S}_{3,5}(\alpha\text{-OAc})$, ac $\text{S}_{3,5}(\alpha\text{-OR})$, $\text{S}_{3,5}(\alpha\text{-OR})$
4	139.4	ac $\text{G}_1(\alpha\text{-OAc})$, $\text{S}_4(\alpha\text{-OR})$
5	137.2	$\text{S}_4(\alpha\text{-OAc})$, ac $\text{S}_1(\alpha\text{-OAc})$, $\text{S}_1(\alpha\text{-OR})$
6	132.1	$\text{G}_1(\alpha\text{-OAc})$
7	129.2	ac $\text{S}_4(\alpha\text{-OAc})$, ac $\text{S}_4(\alpha\text{-OR})$, $\text{H}_{2,6}$
8	123.6	ac $\text{G}_5(\alpha\text{-OAc})$, ac $\text{G}_5(\alpha\text{-OR})$
9	120.3	$\text{G}_6(\alpha\text{-OAc})$ and $\text{G}_6(\alpha\text{-OR})$
10 ^a	113.0	G_2 , ac $\text{G}_2(\alpha\text{-OAc})$
10 ^b	111.1	G_2 , ac $\text{G}_2(\alpha\text{-OR})$
11	105.3	$\text{S}_{2,6}(\alpha\text{-OAc})$, $\text{S}_{2,6}(\alpha\text{-OR})$
12	103.3	$\text{S}_{2,6}$
13	81.0	C_β in $\beta\text{-O-4}$
14	72.7	C_α in $\beta\text{-O-4}$
15	64.1	C_γ in $\beta\text{-O-4}$, $\alpha\text{-o-4}$, $\beta\text{-1}$
16	56.6	CH_3 in methoxyl
17	20.6	CH_3 in acetyl

* G: guaiacyl, S: syringyl, ac: acetylated

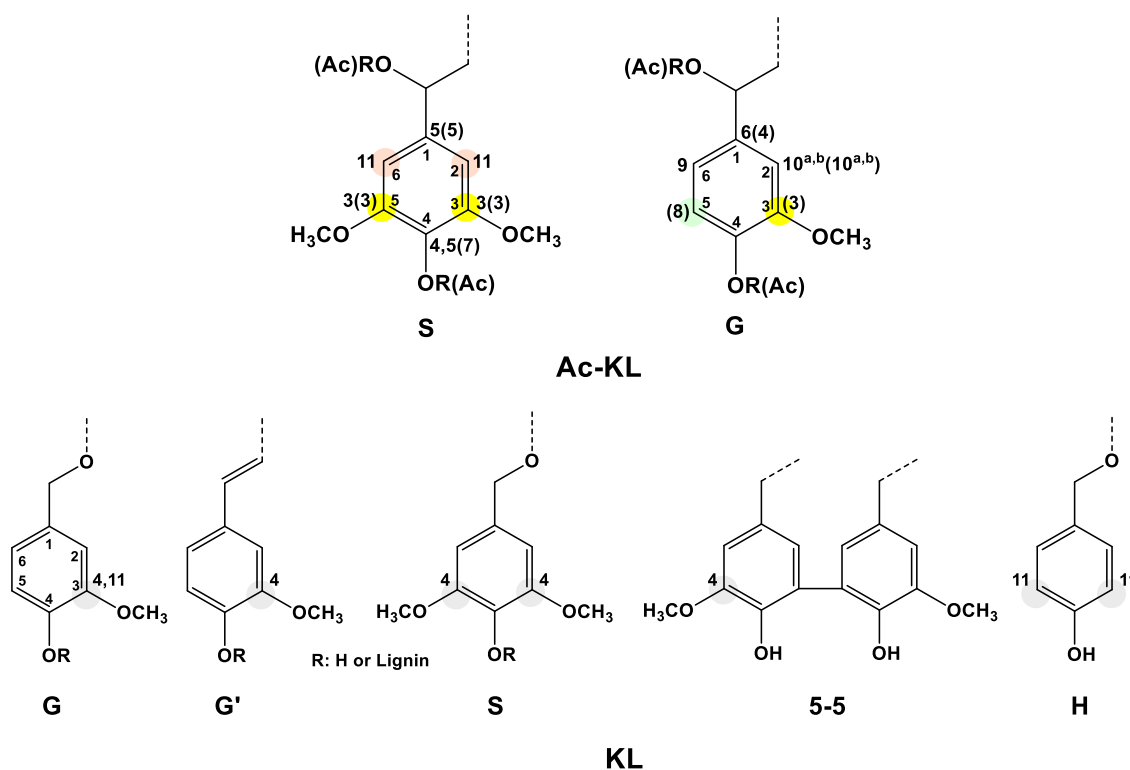


Fig. 2. Substructures of Ac-KL and KL corresponding to ^{13}C NMR assignments

Figure 3 shows the aromatic (140–90/7.9–6.4 ppm) and oxygenated aliphatic (120–70/6.1–4.6 ppm) regions of Ac-KL in 2D HMQC spectrum. The chemical shifts and assignments listed in Table 2 were based on the works of Nimz *et al.* (1981), Balakshin *et al.* (2003), del Río *et al.* (2009), Wen *et al.* (2013b), Eugenio *et al.* (2021), Lahtinen *et al.* (2021), and Wang *et al.* (2022). The substructures present in Ac-KL with their corresponding notations are shown in Fig. 4.

The aromatic region (Fig. 3a) shows S and G-related structures, as well as stilbene. The S moieties ($S_{2,6}$, $S_{2,6'}$, and $S_{2,6''}$) were in the range 106–103/7.3–6.7 ppm. The G moieties were situated in 115–110/7.7–6.9 ppm for C_2 – H_2 in G related structures and 125–118/7.6–6.9 ppm corresponded to the C_6 – H_6 of G units. The C_α -oxidized guaiacyl related structures such as vanillin and acetovanillone were also detected in the spectrum. In addition, the signal around 124.8/7.3–6.8 ppm was assigned to C_6 – H_6 of conjugated carbonyl or carboxyl and 129.2/7.4–7.1 ppm to C – $H_{\alpha\beta}$ of the G unit.

The C_α – H_α in stilbene structures with β -1 (SB1) linkage, and C_α – H_α and C_β – H_β with β -5 (SB5) linkage were identified (Table 2). During kraft pulping, the β -1 moieties (*e.g.* diphenylethanes, spirodienones) generates SB1, while the β -5 moieties can produce SB5 *via* retro-aldol addition reaction (Crestini *et al.* 2017; Giummarella *et al.* 2020).

In the oxygenated aliphatic region (Fig. 3b), β -O-4 moieties (A) were detected. In general, the β -O-4 linkage, comprising about 60% in hardwood lignins, is extensively cleaved due to the nucleophilic attack of SH^- and OH^- during kraft pulping. However, the C_α – H_α (75.4/6.02 ppm) and C_β – H_β (80.4/4.6 ppm) of A were detected in HMQC spectrum. This suggests that there were small amounts of β -O-4 bonds uncleaved during kraft pulping. The β - β moieties (B) in 86.6/4.76 ppm were also detected.

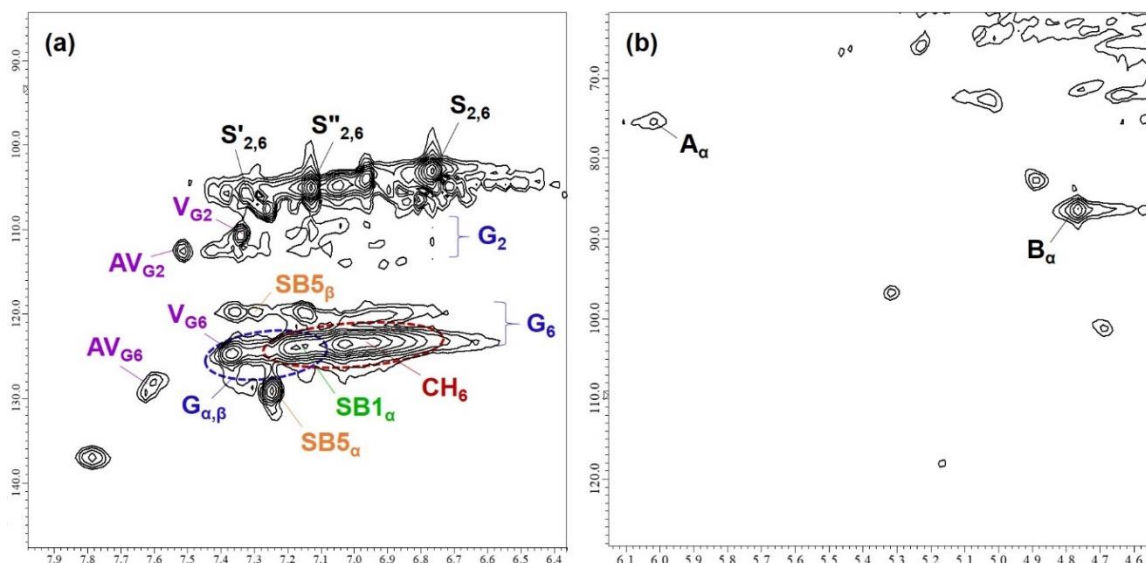


Fig. 3. Aromatic (a) and oxygenated aliphatic (b) region of the HMQC spectra of Ac-KL

Table 2. Assignments of ^{13}C – ^1H Correlation Signals in HMQC Spectra of Ac-KL

Label	$\delta_{\text{C}}/\delta_{\text{H}}$ (ppm)	Assignments
	20.2/2.23	Aliphatic acetyl
	30.5/1.29	Aromatic acetyl
OCH ₃	56.3/3.80	C–H in methoxyls
A _α	75.4/6.02	C _α –H _α in β-O-4 (A)
B _α	86.6/4.76	C _α –H _α in β-β resinol (B)
S _{2,6}	103.3/6.76	C _{2,6} –H _{2,6} in syringyl units (S)
S'' _{2,6}	105.0/7.13	C _{2,6} –H _{2,6} in oxidized (C _α OOH) syringyl units (S'')
S' _{2,6}	105.8/7.33	C _{2,6} –H _{2,6} in oxidized (C _α =O) syringyl units (S')
G ₂	115–110/7.5–6.9	C ₂ –H ₂ in guaiacyl related units (G)
V _{G2}	110.8/7.34	C ₂ –H ₂ in vanillin units (V)
AV _{G2}	112.6/7.51	C ₂ –H ₂ in acetovanillone units (AV)
G ₆	125–118/7.6–6.9	C ₆ –H ₆ in guaiacyl related units (G)
SB5 _β	120.1/7.28	C _β –H _β in stilbene, β-5 (SB5)
V _{G6}	124.7/7.37	C ₆ –H ₆ in vanillin units (V)
AV _{G6}	128.8/7.61	C ₆ –H ₆ in acetovanillone units (AV)
SB1 _α	124.0/7.17	C _α –H _α in stilbene, β-1 (SB1)
CH ₆	124.8/7.3–6.8	C ₆ –H ₆ in conjugated CO or COOH
G _{α,β}	128.5/7.4–7.1	C–H _{α/β} in guaiacyl units (G)
SB5 _α	129.1/7.25	C _α –H _α in stilbene, β-5 (SB5)

The structural changes caused by kraft pulping were confirmed by 2D HMQC NMR result of Ac-KL. Some structures such as stilbene and vanillin, which were not observed previously by 1D NMR analysis, were confirmed by 2D HMQC NMR.

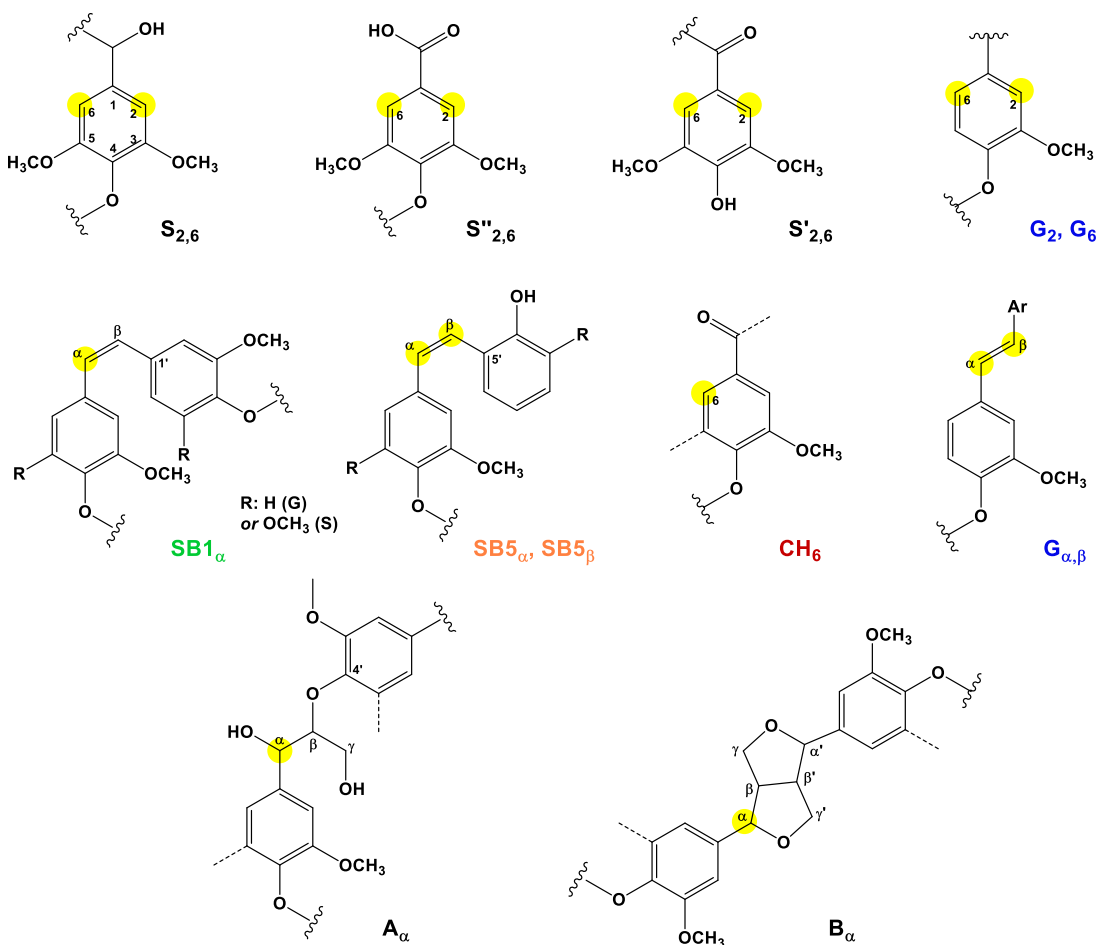


Fig. 4. Substructures present in Ac-KL from 2D HMQC NMR

³¹P NMR Analysis

The hydroxyl and carboxyl content of KL were determined through the ³¹P NMR protocol based on Meng *et al.* (2019) and Argyropoulos *et al.* (2021). Based on qualitative and quantitative analysis of hydroxyl groups in lignin model compounds (Archipov *et al.* 1991) and various types of lignin (Argyropoulos *et al.* 1993a), different types of hydroxyl groups such as aliphatic and phenolic hydroxyl groups – even the guaiacyl (G), syringyl (S), *p*-hydroxyphenyl (H), and C5 condensed phenolic hydroxyl groups – can be quantified by simply comparing the integrals of sample peaks to an internal standard (Argyropoulos *et al.* 2021). N-hydroxy-5-norbornene-2,3-dicarboximide (NHND) was used as an internal standard since NHND is baseline resolved from lignin-derived resonances (Zawadzki and Ragauskas 2001). Simply, its lone hydroxyl group does not overlap with any of the hydroxyl groups originating from the sample. In addition, the quantification of carboxylic acid group in KL is possible with NHND. Chromium (III) acetylacetonate was also added as a relaxation agent to speed up the ³¹P spin-lattice relaxation behavior of phosphitylated samples (Argyropoulos *et al.* 1993b).

For a reliable determination of hydroxyl groups present in KL by ³¹P NMR, there are two important factors to be considered. First, the KL sample must completely be dissolved in the pyridine/CDCl₃ solvent. Second, there should be no presence of water in the sample. The presence of water in the sample destroys the phosphitylating agent, 2-

chloro-4,4,5,5-tetramethyl-1,3,2-dioxaphospholane, and produces 2-hydroxy-4,4,5,5-tetramethyl-1,3,2-dioxaphospholane, which is a yellow precipitate. Any formation of precipitate leads to non-homogeneity of the sample being analyzed, which makes the sample not suitable for analysis. In this study, KL was completely dissolved in the solvent and was ensured to be free of moisture.

Figure 5 (a) shows the full ^{31}P NMR spectrum of phosphitylated KL and (b) shows the enlarged hydroxyl group region of interest (150–134 ppm). A sharp peak at 174 ppm was due to the excess amount of unreacted TMDP. The presence of an excess amount of TMDP indicated that all hydroxyl groups in KL were completely derivatized.

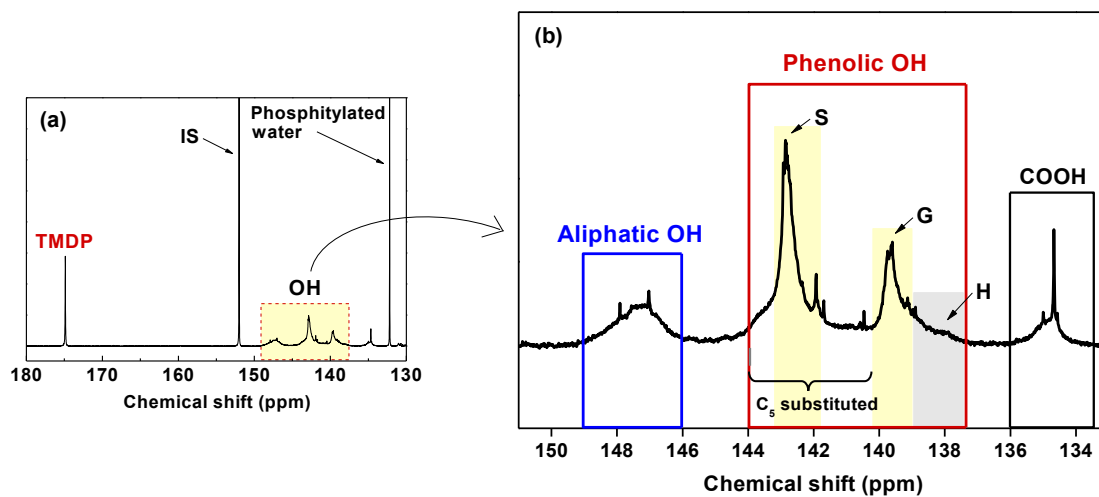


Fig. 5. ^{31}P NMR spectrum (a) and enlarged spectrum (b) of KL. S: syringyl, G: guaiacyl, H: *p*-hydroxyphenyl

The aliphatic and phenolic (S, G, H) hydroxyl, and carboxyl contents of KL calculated from the ^{31}P NMR result are listed in Table 3. The hydroxyl content was compared to modified and commercial KLs from published data (Cateto *et al.* 2008; Sameni *et al.* 2016; Antonino *et al.* 2021). For the KL used in this study, which was provided by Moorim P&P – the only kraft mill in Korea, the total hydroxyl content was found to be 5.24 mmol/g KL. The total hydroxyl content of KL in this study was similar to the KL derived from hardwood in alkaline condition (5.14 mmol/g KL). The total hydroxyl content was remarkably lower compared to Indulin AT, a commercial KL from softwoods. This suggests that softwood KL has higher hydroxyl content than hardwood KL. The phenolic hydroxyl content was not remarkably different between hardwood and softwood KLs, however the aliphatic hydroxyl content was relatively lower in hardwood KLs than softwood.

The phenolic hydroxyl content was higher than aliphatic hydroxyl content for each of the KLs listed. This result agreed with the result of ^1H NMR analysis from the study of Mun *et al.* (2021) (Fig. 6). This indicated that the cleavage of β -O-4 and α -O-4 bonds during the kraft pulping process and creation of new phenolic hydroxyl groups in etherified lignin (Sameni *et al.* 2016).

Table 3. Hydroxyl and Carboxyl Content of KL

Lignin Functionality	Amount (mmol/g KL)				
	Mixed KL ^a (hardwood)	Acid KL ^b (hardwood)	Alkali KL ^b (hardwood)	Indulin AT ^c (softwood)	Indulin AT ^d (softwood)
Aliphatic OH	1.04	1.11	1.00	2.34	2.59
Phenolic OH	4.20	4.50	4.14	4.11	4.00
Syringyl OH	1.02	2.28	2.05	0.33	
Guaiacyl OH	0.97	2.10	1.97	1.96	
<i>p</i> -hydroxyphenyl OH	0.30	0.13	0.13	0.26	
*Total OH	5.24	5.61	5.14	6.85	6.59
COOH	0.44				0.20

*Total OH = aliphatic OH + aromatic OH;

^aThis study, ^bAntonino *et al.* 2021, ^cCateto *et al.* 2008, ^dSameni *et al.* 2016

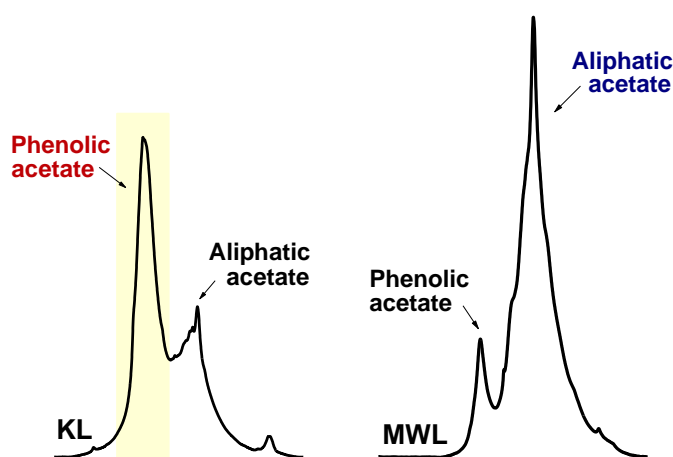


Fig. 6. Comparison of aromatic/aliphatic regions of KL and MWL from ¹H NMR (Mun *et al.* 2021).

Of the phenolic hydroxyl groups, the contribution of S and G was 1.02 and 0.97 mmol/g KL, respectively. The S/G molar ratio of KL determined *via* ³¹P NMR method was 1.05, which was similar to the hardwood acid (1.09) and alkali (1.04) KL (Antonino *et al.* 2021). In addition, it had similar tendency with the S/G ratio obtained from ¹H NMR (1.13) in the authors' previous study (Mun *et al.* 2021).

The region around 143.0–140.2 ppm is for C₅ substituted phenolic hydroxyl group (Balakshin and Capanema 2015). Due to the signal overlapping between 5-substituted phenolics (S units and various 5-condensed G units), overestimation of S and underestimation of condensed units can occur in hardwood KLs (Meng *et al.* 2019). In KL, 5-substituted phenolics not only represent 4-O-5, β-5, 5-5 but also stilbenes with β-5 linkage (Lancefield *et al.* 2018). The C₅ substituted hydroxyl content of mixed hardwood KL was 2.21 mmol/g KL. The S hydroxyl content (1.02 mmol/g KL) was subtracted from C₅ substituted phenolic hydroxyl content (2.21 mmol/g), which gives 5-condensed hydroxyl content (1.19 mmol/g KL).

In mixed hardwood KL, the H hydroxyl content (0.30 mmol/g KL) and carboxyl content (0.44 mmol/g KL) were relatively lower than their aliphatic, C₅ substituted phenolic, S and G hydroxyl counterparts.

CONCLUSIONS

1. From 2D HMQC NMR analysis of kraft lignin (KL) from mixed hardwoods, lignin substructures such as stilbene (β -1 and β -5) and vanillin were confirmed. These substructures were previously not detected in 1D NMR but were confirmed in 2D NMR.
2. The syringyl and guaiacyl moieties in KL were detected in the aromatic region, while trace amounts of β -O-4 and β - β moieties were detected in the oxygenated aliphatic region.
3. The total hydroxyl content calculated from ^{31}P NMR was 5.24 mmol/g KL, and the phenolic hydroxyl content (4.20 mmol/g KL) was higher than aliphatic hydroxyl content (1.04 mmol/g KL).
4. The S/G molar ratio of KL calculated from ^{31}P NMR was 1.05 (S: 1.02 mmol/g KL, G: 0.97 mmol/g KL).
5. The carboxyl content was 0.44 mmol/g KL.

ACKNOWLEDGMENTS

This research was supported by the National Research Foundation of Korea (NRF) grant funded by the Korean government (MSIT) (No. 2020R1A2C2012356). The authors would like to appreciate Moorim P&P for providing kraft lignin and CURF, JBNU for the technical assistance.

REFERENCES CITED

- Antonino, L. D., Gouveia, J. R., de Sousa Júnior, R. R., Garcia, G. E. S., Gobbo, L. C., Tavares, L. B., and Dos Santos, D. J. (2021). "Reactivity of aliphatic and phenolic hydroxyl groups in kraft lignin towards 4,4' MDI," *Molecules* 26(8), 2131. DOI: 10.3390/molecules26082131
- Archipov, Y., Argyropoulos, D. S., Bolker, H. I., and Heitner, C. (1991). " ^{31}P NMR spectroscopy in wood chemistry. Part I. Model compounds," *J. Wood Chem. Technol.* 11(2), 137-157. DOI: 10.1080/02773819108050267
- Argyropoulos, D. S., Bolker, H. I., Heitner, C., and Archipov, Y. (1993a). " ^{31}P NMR spectroscopy in wood chemistry part V. Qualitative analysis of lignin functional groups," *J. Wood Chem. Technol.* 13(2), 187-212. DOI: 10.1080/02773819308020514
- Argyropoulos, D. S., Bolker, H. I., Heitner, C., and Archipov, Y. (1993b). " ^{31}P NMR spectroscopy in wood chemistry. Part IV. Lignin models: Spin lattice relaxation times and solvent effects in ^{31}P NMR," *Holzforschung* 47(1), 50-56. DOI: 10.1515/hfsg.1993.47.1.50
- Argyropoulos, D. S., Pajer, N., and Crestini, C. (2021). "Quantitative ^{31}P NMR analysis of lignins and tannins," *J. Vis. Exp.* 174, e62696. DOI: 10.3791/62696
- Balakshin, M. Y., Capanema, E. A., Chen, C. L., and Gracz, H. S. (2003). "Elucidation of the structures of residual and dissolved pine kraft lignins using an HMQC NMR

- technique,” *J. Agric. Food Chem.* 51(21), 6116–6127. DOI: 10.1021/jf034372d
- Balakshin, M., and Capanema, E. (2015). “On the quantification of lignin hydroxyl groups with ^{31}P and ^{13}C NMR spectroscopy,” *J. Wood Chem. Technol.* 35(3), 220-237. DOI: 10.1080/02773813.2014.928328
- Cateto, C. A., Barreiro, M. F., Rodrigues, A. E., Brochier-Solan, M. C., Thielemans, W., and Belgacem, M. N. (2008). “Lignins as macromonomers for polyurethane synthesis: A comparative study on hydroxyl group determination,” *J. Appl. Polym. Sci.* 109(5), 3008-3017. DOI: 10.1002/app.28393
- Crestini, C., Lange, H., Sette, M., and Argyropoulos, D. S. (2017). “On the structure of softwood kraft lignin,” *Green Chem.* 19(17), 4104-4121. DOI: 10.1039/C7GC01812F
- del Río, J. C., Rencoret, J., Marques, G., Li, J., Gellerstedt, G., Jiménez-Barbero, J., Martínez, A. T., and Gutiérrez, A. (2009). “Structural characterization of the lignin from jute (*Corchorus capsularis*) fibers,” *J. Agric. Food Chem.* 57(21), 10271-10281. DOI: 10.1021/jf900815x
- Eugenio, M. E., Martín-Sampedro, R., Santos, J. I., Wicklein, B., and Ibarra, D. (2021). “Chemical, thermal and antioxidant properties of lignins solubilized during soda/AQ pulping of orange and olive tree pruning residues,” *Molecules* 26(13), 3819. DOI: 10.3390/molecules26133819
- Goldschmid, O. (1954). “Determination of phenolic hydroxyl content of lignin preparations by ultraviolet spectrophotometry,” *Anal. Chem.* 26(9), 1421-1423. DOI: 10.1021/ac60093a009
- Giummarella, N., Pylypchuk, I. V., Sevastyanova, O., and Lawoko, M. (2020). “New structures in *Eucalyptus* kraft lignin with complex mechanistic implications,” *ACS Sustainable Chem. Eng.* 8(29), 10983-10994. DOI: 10.1021/acssuschemeng.0c03776
- Guterres, A. (2020). “Carbon neutrality by 2050 is the world’s most urgent mission,” (<http://www.unrcca.unmissions.org>), accessed 27 June 2022.
- Jardim, J. M., Hart, P. W., Lucia, L., and Jameel, H. (2020). “Insights into the potential of hardwood kraft lignin to be a green platform material for emergence of the biorefinery,” *Polymers* 12(8), 1795. DOI: 10.3390/polym12081795
- Katahira, R., Elder, T. J., and Beckham, G. T. (2018). “A brief introduction to lignin structure,” in: *Lignin Valorization: Emerging Approaches*, The Royal Society of Chemistry, pp. 1–9.
- Lahtinen, M. H., Mikkilä, J., Mikkonen, K. S., and Kilpeläinen, I. (2021). “Kraft process – Formation of secoisolariciresinol structures and incorporation of fatty acids in kraft lignin,” *J. Agric. Food Chem.* 69(21), 5955-5965. DOI: 10.1021/acs.jafc.1c00705
- Lancefield, C. S., Wienk, H. L. J., Boelens, R., Weckhuysen, B. M., and Bruijninx, P. C. A. (2018). “Identification of a diagnostic structural motif reveals a new reaction intermediate and condensation pathway in kraft lignin formation,” *Chem. Sci.* 9(30), 6348-6360. DOI: 10.1039/C8SC02000K
- Meng, X., Crestini, C., Ben, H., Hao, N., Pu, Y., Ragauskas, A. J., and Argyropoulos, D. S. (2019). “Determination of hydroxyl groups in biorefinery resources via quantitative ^{31}P NMR spectroscopy,” *Nature Protocols* 14, 2627-2647. DOI: 10.1038/s41596-019-0191-1
- Mun, J. S., Pe, J. A., and Mun, S. P. (2021). “Chemical characterization of kraft lignin prepared from mixed hardwoods,” *Molecules* 26(16), 4861. DOI: 10.3390/molecules26164861
- Nimz, H. H., Robert, D., Faix, O., and Nemr, M. (1981). “Carbon -13 NMR spectra of lignins, 8, Structural differences between lignins of hardwoods, softwoods, grasses

- and compression wood,” *Holzforschung* 35(1), 16-26. DOI: 10.1515/hfsg.1981.35.1.16
- Ralph, J., Brunow, G., and Boerjan, W. (2007). “Lignins,” in: *Encyclopedia of Life Sciences*, John Wiley & Sons, Hoboken, NJ, USA, pp. 1-10.
- Sameni, J., Krigstin, S., and Sain, M. (2016). “Characterization of lignins isolated from industrial residues and their beneficial uses,” *BioResources* 11(4), 8435-8456. DOI: 10.1515/hfsg.1981.35.1.16
- Vishtal, A., and Kraslawski, A. (2011). “Challenges in industrial applications of technical lignins,” *BioResources* 6(3), 3547-3568. DOI: 10.15376/biores.6.3.3547-3568
- Wang, J., Zhao, C., Zhang, T., Yang, L., Chen, H., and Yue, F. (2022). “In-depth identification of phenolics fractionated from Eucalyptus kraft lignin,” *Adv. Sustain. Syst.* 6(5), 2100406. DOI: 10.1002/adsu.202100406
- Wen, J. L., Sun, S. L., Xue, B. L., and Sun, R. C. (2013a). “Recent advances in characterization of lignin polymer by solution-state nuclear magnetic resonance (NMR) methodology,” *Materials (Basel)* 6(1), 359-391. DOI: 10.3390/ma6010359
- Wen, J. L., Sun, S. L., Xue, B. L., and Sun, R. C. (2013b). “Quantitative structural characterization of the lignins from the stem and pith of bamboo (*Phyllostachys pubescens*),” *Holzforschung* 67(6), 613-627. DOI: 10.1515/hf-2012-0162
- Zawadzki, M., and Ragauskas, A. (2001). “N-hydroxy compounds as new internal standards for the ³¹P NMR determination of lignin hydroxy functional groups,” *Holzforschung* 55(3), 283-285. DOI: 10.1515/HF.2001.047
- Zhao, X. H., Zhang, Y. j., Wei, L. P., Hu, H. Y., Huang, Z. Q., Yang, M., Huang, A. M., Wu, J., and Feng, Z. F. (2017). “Esterification mechanism of lignin with different catalysts based on lignin model compounds by mechanical activation-assisted solid-phase synthesis,” *RSC Adv.* 7(83), 52382-52390. DOI: 10.1039/c7ra10482k

Article submitted: July 19, 2022; Peer review completed: August 21, 2022; Revised version received: August 26, 2022; Accepted: October 7, 2022; Published: October 14, 2022.
DOI: 10.15376/biores.17.4.6626-6637